Informes Técnicos Ciemat

900

septiembre, 1999

Modification of the Heating Position Using a Moveable Mirror in the TJ-II ECRH System

A. Cappa
V. Tribaldos
K. Likin
A. Fernández
R. Martín

Asociación EURATOM/CIEMAT para Fusión - 59

Departamento de Fusión y Partículas Elementales

Toda correspondenica en relación con este trabajo debe dirigirse al Servicio de Información y Documentación, Centro de Investigaciones Energéticas, Medioambientales y Tecnológicas, Ciudad Universitaria, 28040-MADRID, ESPAÑA.

Las solicitudes de ejemplares deben dirigirse a este mismo Servicio.

Los descriptores se han seleccionado del Thesauro del DOE para describir las materias que contiene este informe con vistas a su recuperación. La catalogación se ha hecho utilizando el documento DOE/TIC-4602 (Rev. 1) Descriptive Cataloguing On-Line, y la clasificación de acuerdo con el documento DOE/TIC.4584-R7 Subject Categories and Scope publicados por el Office of Scientific and Technical Information del Departamento de Energía de los Estdos Unidos.

Depósito Legal: M -14226-1995
ISSN: 1135 - 9420
NIPO: 238-99-003-5

Editorial CIEMAT

CLASIFICACIÓN DOE Y DESCRIPTORES

700340
PLASMA HEATING; MIRRORS; ECR HEATING; CURRENT-DRIVE HEATING; TOKAMAK DEVICES

"Modification of the Heating Position Using a Moveable Mirror in the TJ-II ECRH System"

Cappa, A.; Tribaldos, V.; Likin, K.; Fernández, A.; Martín, R.
23 pp. 13 fig. 5 refs.

Abstract:

During the first stages of operation, start-up and heating of plasmas in TJ-II stellerator are being produced by EC waves. These are launched by two ½-MW type gyrotrons at 53.2 GHz and transmitted to the plasma by two quasi-optical transmission lines located at two symmetrical stellarator positions. The last mirror of both lines, placed inside the vacuum vessel, is a moveable mirror allowing for changes in the final direction of the microwave beam and therefore in the heating position. This report is devoted to the calculations describing the movement of this mirror and its influence in the position of the reflected beam.

"Modificación de la Posición de Calentamiento Mediante un Espejo Móvil en el Sistema ECRH del Stellarator TJ-II."

Cappa, A.; Tribaldos, V.; Likin, K.; Fernández, A.; Martín, R.
23 pp. 13 fig. 5 refs.

Resumen:

Durante las primeras etapas de funcionamiento, la creación y el calentamiento de los plasmas producidos en el stellarator TJ-II se consigue mediante la inyección de ondas electromagnéticas con una frecuencia de 53.2 GHz (ECR). Estas son lanzadas por dos girotrones de clase ½-MW y conducidas al plasma por dos líneas de transmisión cuasi-ópticas colocadas en dos posiciones simétricas de TJ-II. El último espejo de ambas líneas, localizado en el interior de la cámara de vacío, es un espejo móvil que permite cambiar la dirección final del haz de microondas y por lo tanto la posición del punto de calentamiento. Este informe está dedicado a los cálculos que describen el movimiento de este espejo así como su influencia en la posición del haz reflejado.

1.Introduction

The ECRH system transmission lines of the TJ-II stellarator have been designed to provide a large flexibility in the heating position. The complex geometry of TJ-II, far away from the toroidal symmetry of tokamaks, makes it desirable the possibility of change the injected beam direction, not only for optimization of the heating itself, by achieving narrow and localized power deposition profiles, but also for using the ECRH as an experimental and diagnostic tool. In particular, localized currents can be induced with different intensities and direction, depending on the value of the parallel index of refraction. Thereby it is possible to control the rotational transform profile or to compensate the bootstrap currents. Moreover the fraction of trapped particles interacting with the beam can be modified and its influence on heating can be studied.

In TJ-II, these requirements are accomplished with a moveable elliptical mirror placed at the end of each transmission line. Both mirrors are located inside the vacuum vessel, at symmetrical stellarator positions and are handled independently by two external drives. By changing the mirror position, given by two angles, the beam can be pointed in the desired direction and hit the plasma at any chosen point within its range. The main problem is to know the output direction of the reflected beam for given values of the positioning angles of the mirror. This is not immediate because the design requirements issued from a lack of space inside the vessel introduce a dependence on the angles of the position of the mirror. The calculations presented in this report are related only with the geometry and design of the internal moveable mirror and they can be applied to both mirrors by taking in account the stellarator symmetry. More detailed information about the ECRH system and the underlying physics can be found in the references [1,2,3] and [4] respectively.

The organization of this report is as follows. In Section 2 the current design of the transmission lines is presented and the internal mirror and its movement are described. The main calculations are presented in Section 3 where the equation describing the mirror surface for arbitrary values of its positioning angles is obtained. Then, the normal vector to this surface is calculated and the final direction of the reflected beam is obtained as a function of the positioning angles. As mentioned above, we want to know the values of the angles for a given output direction. This is achieved by the numerical minimization of a functional of the angles. Section 4 shows as an example the results obtained from Section3 when heating on-axis is desired. The mirror calibration and the measurements done in laboratory are described in Section 5. Finally, in Appendix 1, we recalculate the transformation matrix M, introduced in Section 3 to obtain the general equation of the mirror surface, using a different approach from the one presented in that section.

2.Transmission lines and internal mirror

The two quasi-optical transmission lines consist of a set of focusing aluminum mirrors plus one last moveable mirror located inside the vacuum vessel of TJ-II. The lines are located at two symmetrical stellarator positions. The first line launches the microwaves in the horizontal plane through the side port of the A6 sector (at $\varphi_{A6} = 64.53°$, z = 490 mm) with a small angle $\alpha = 8.37°$ in respect to the machine radial direction whereas the second one uses the B3 sector (at $\varphi_{B3} = 115.47°$, z = −490 mm) with analogue conditions. Figure 1 outlines the ECRH system of TJ-II and its basic characteristics.

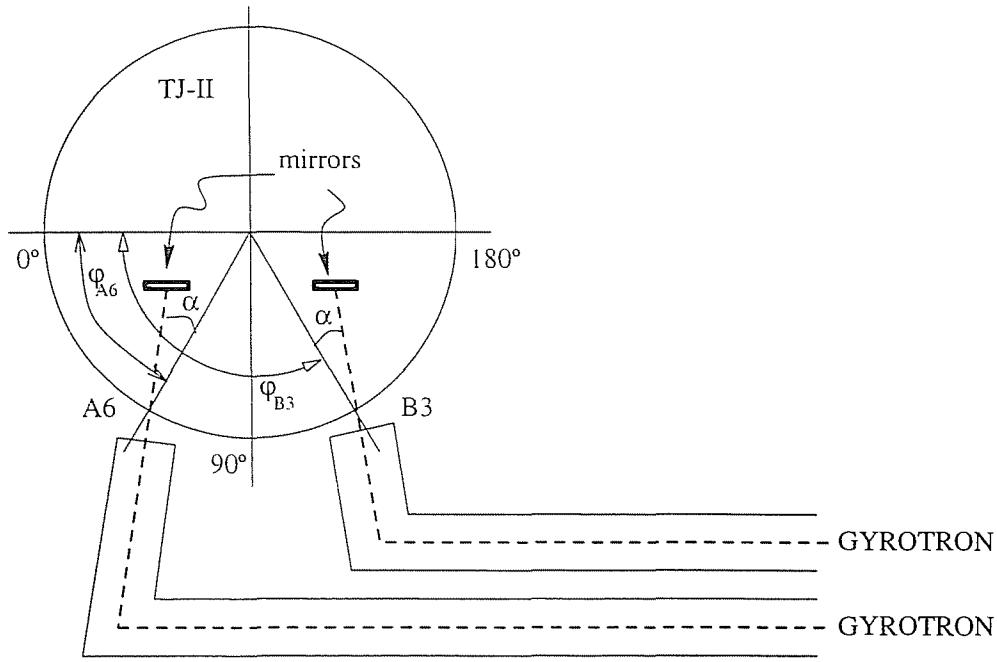

Figure 1. The TJ-II ECRH system

The stellarator symmetry ($\psi\ (R, \pi/4 + \varphi, z) = \psi\ (R, \pi/4 - \varphi, -z)$), together with the fact that the lines are placed at symmetrical stellarator positions reduces the study to one single line. From now on we will consider the first transmission line located at the A6 sector.

The internal mirror is an elliptical mirror (with size 170 mm x 190 mm) also placed on the A6 sector. Its position is given by two rotation angles a_1 (toroidal angle), and a_2 (poloidal angle). Figure 2 shows the mirror position for arbitrary values of the angles a_1 and a_2 (the positive rotation direction is indicated for both angles).

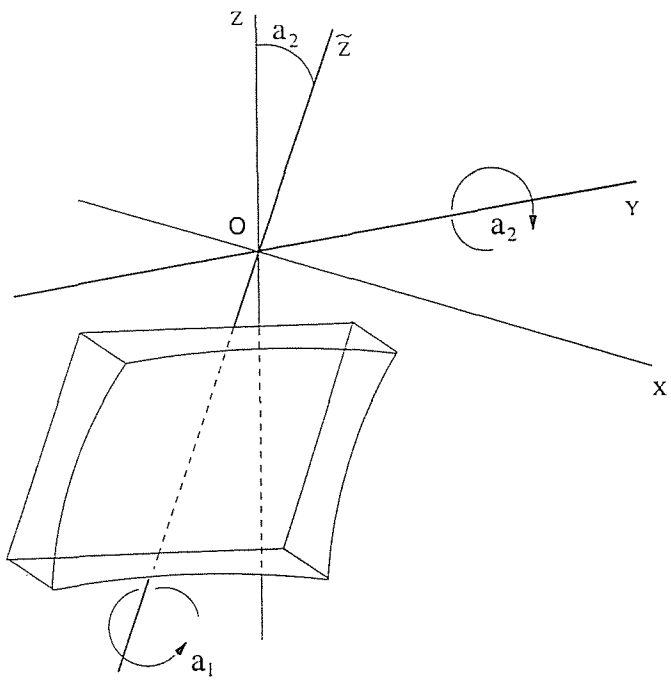

Figure 2. Mirror movement

The movement of the mirror is such that the position of the mirror itself , and not only its orientation, depends on the values of the angles.

It is important to note that the two axis of rotation are not equivalent. One of them belongs to the mirror and follows its movement, we call it $\tilde{z}$ (see Figure 2). The other one is fixed and corresponds to the y reference axis. The main calculations will be referred to a spatial point O, not located in the mirror and invariant under the two rotations, that is, a fixed point. When both angles are zero, the equation defining the mirror surface in the fixed point reference system is the equation of an ellipsoid centered at (d = 396 mm, 0, $-c$ = −135 mm) with half-major axis a = 445 mm and half-minor axis b = 393 mm.

$$S(x,y,z)=\frac{(x-d)^2+y^2}{b^2}+\frac{(z+c)^2}{a^2}-1=0 \qquad (1)$$

a = 445 mm $\quad$ c = 135 mm
b = 393 mm $\quad$ g = 3 mm
$d = b + g$

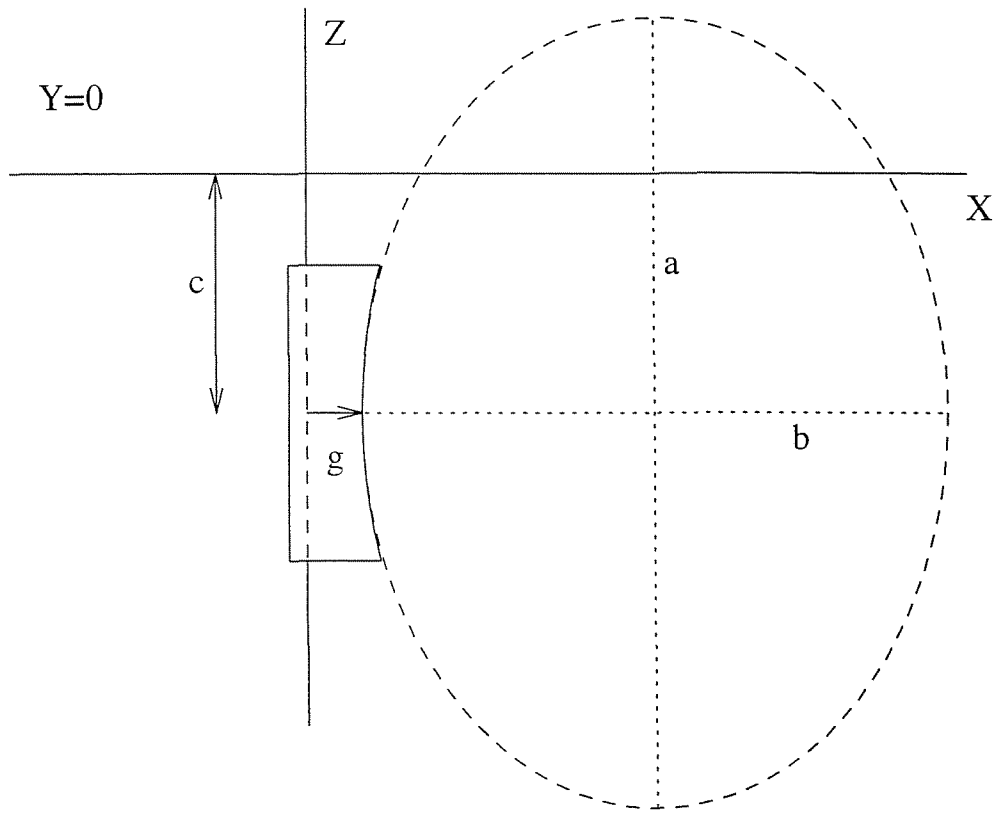

Figure 3. Mirror parameters

The mirror is handled from the upper side of the port by two mechanical vacuum drives, a rotary drive for the toroidal angles and a linear drive for the poloidal angles. Both drives are installed in the window flange. A detailed view of the mirror and its position respect to the vacuum vessel is shown at the end of the report.

3.Beam reflection

As stated in Section 2 the mirror is able, by changing the values of the positioning angles with the drives, to send the reflected beam in different directions. The main problem is, given a desired heating point, to find the angles for which the mirror reflects the beam towards this point. Figure 4 shows the parameters involved in the calculation.

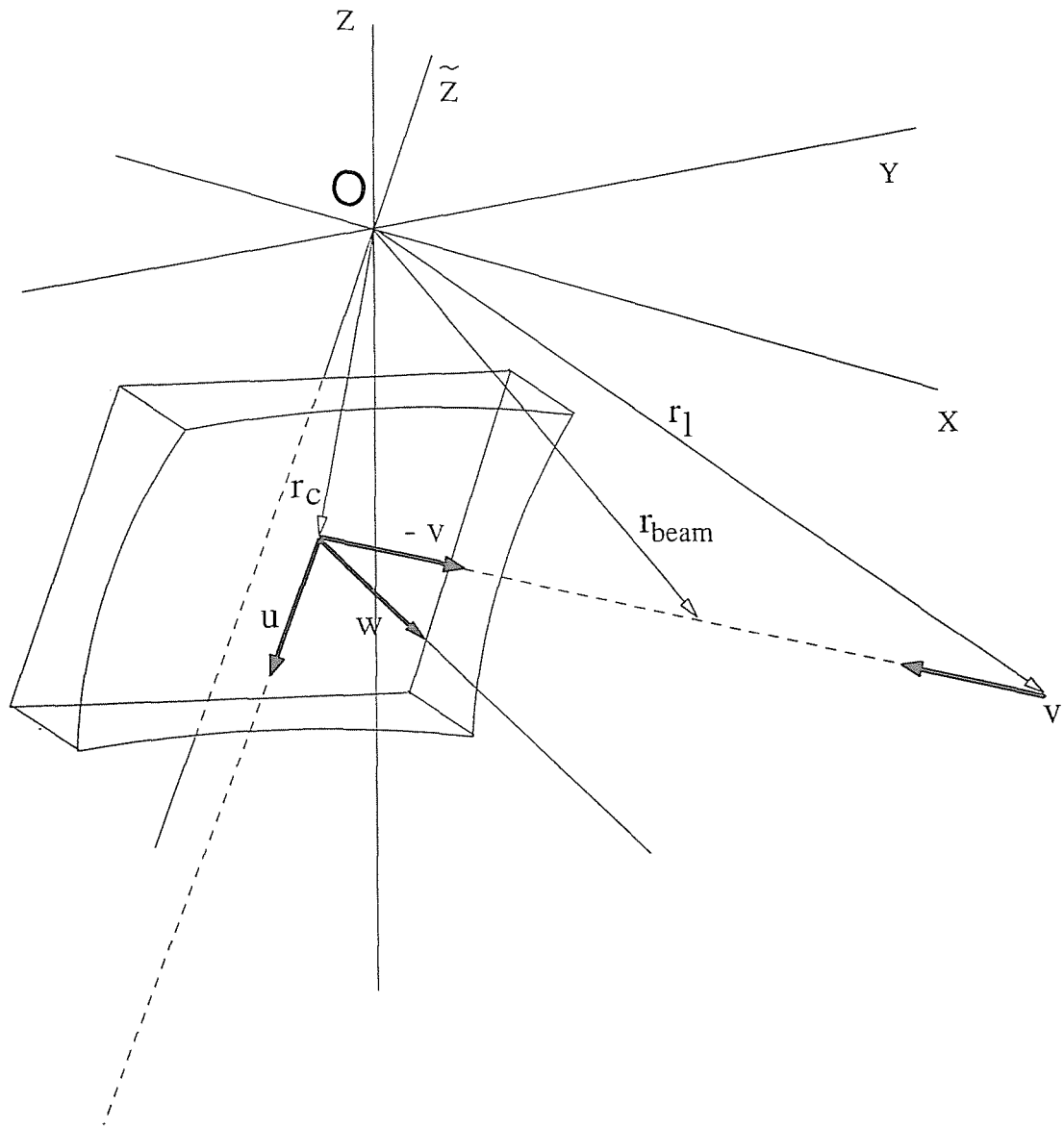

Figure 4. Beam reflection parameters

Where v ($|v| = 1$) is the director vector of the injected beam, r_l the launching point, r_c is the reflection point and w ($|w| = 1$) is the vector perpendicular to the surface at this point. The components of the beam vectors v and r_l referred to O are:

$v_x = -\cos\alpha$	$r_{lx} = 895{,}5$ mm
$v_y = -\sin\alpha$	$r_{ly} = 140$ mm
$v_z = 0$	$r_{lz} = -123{,}9$ mm

with $\alpha = 8.37°$

The vector $\boldsymbol{u}$ ($|\boldsymbol{u}| = 1$) is the director vector of the reflected beam and can be calculated taking into account the fact that the reflection only changes the sign of the component of $\boldsymbol{v}$ parallel to vector $\boldsymbol{w}$.

$$\boldsymbol{u} = -2(\boldsymbol{w} \cdot \boldsymbol{v})\boldsymbol{v} + \boldsymbol{v} \tag{2}$$

Thus, the direction of the reflected beam is determined when the point of the mirror where reflection takes place and the normal vector at this point are known. The normal vector to the mirror surface is obtained by taking the partial derivatives in the general equation of the mirror surface (for any values of the angles a_1 and a_2). The reflection point $\boldsymbol{r}_c$ is the intersection point between this surface and the injected beam with direction given by $\boldsymbol{v}$. In both cases the equation of the transformed surface as a function of the rotation angles is necessary.

Let $\boldsymbol{r}$ be an arbitrary vector in the fixed point reference system. The transformed vector $\tilde{r}$ is the result of two consecutive rotations, a rotation R_1 with angle a_1 around the z axis (see Figure 5) and a rotation R_2 with angle a_2 around the y axis (see Figure 6). Both rotations define the movement of the mirror.

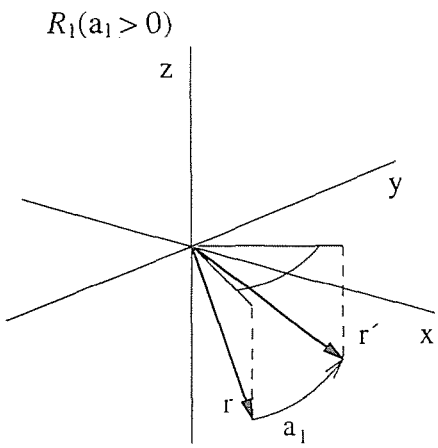

Figure 5. Rotation around the z axis

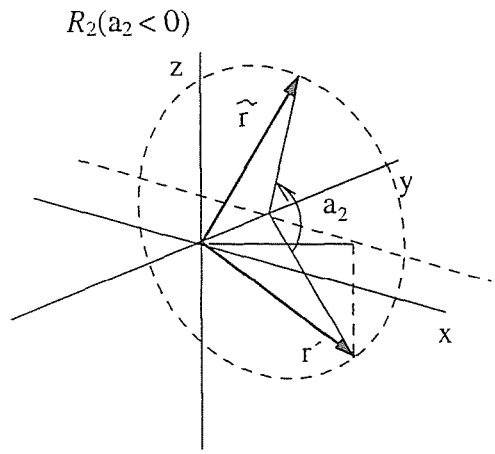

Figure 6. Rotation around the y axis

M_1 represents the rotation R_1:

$$\overbrace{\begin{pmatrix} x' \\ y' \\ z' \end{pmatrix}}^{\boldsymbol{r}'} = \overbrace{\begin{pmatrix} \cos a_1 & -\sin a_1 & 0 \\ \sin a_1 & \cos a_1 & 0 \\ 0 & 0 & 1 \end{pmatrix}}^{M_1} \overbrace{\begin{pmatrix} x \\ y \\ z \end{pmatrix}}^{\boldsymbol{r}}$$

and M_2 represents the rotation R_2:

$$\overbrace{\begin{pmatrix} \tilde{x} \\ \tilde{y} \\ \tilde{z} \end{pmatrix}}^{\tilde{\boldsymbol{r}}} = \overbrace{\begin{pmatrix} \cos a_2 & 0 & \sin a_2 \\ 0 & 1 & 0 \\ -\sin a_2 & 0 & \cos a_2 \end{pmatrix}}^{M_2} \overbrace{\begin{pmatrix} x' \\ y' \\ z' \end{pmatrix}}^{\boldsymbol{r}'}$$

Therefore,

$$\tilde{r} = M_2 r' = M_2 M_1 r = Mr \tag{3}$$

where

$$M = \begin{pmatrix} \cos a_1 \cos a_2 & -\sin a_1 \cos a_2 & \sin a_2 \\ \sin a_1 & \cos a_1 & 0 \\ -\cos a_1 \sin a_2 & \sin a_1 \sin a_2 & \cos a_2 \end{pmatrix}$$

The final physical result must be the same independently of the order chosen for the rotations. It is obvious that, physically, nothing changes if we manipulate first the rotary drive and then the linear drive or first the linear drive and then the rotary drive. Nevertheless the matrix representing these rotations are not the same when the rotations order is changed. If we apply the rotations in the inverse order, the matrix representing R_2 does not change but the matrix for R_1 is no longer the same. The new matrix is more complicated since the rotation is now around the $\tilde{z}$ axis, transformed of z by R_2. This matrix is calculated in Appendix 1.

If $\boldsymbol{r}$ verifies (1) then $\tilde{r}$ belongs to the transformed surface $\tilde{S}$, thus, from equation (3)

$$\boldsymbol{r} = M^{-1}\tilde{r} \tag{4}$$

and

$$S(\boldsymbol{r}) = S(M^{-1}\tilde{r}) \equiv \tilde{S}(\tilde{r}) \equiv \Phi(\tilde{r})$$

where the inverse of matrix M is

$$M^{-1} = \begin{pmatrix} \cos a_1 \cos a_2 & \sin a_1 & -\cos a_1 \sin a_2 \\ -\sin a_1 \cos a_2 & \cos a_1 & \sin a_1 \sin a_2 \\ \sin a_2 & 0 & \cos a_2 \end{pmatrix}$$

Introducing (4) in (1) we obtain the equation of the mirror surface as a function of the angles a_1 and a_2 in the fixed point reference system, namely

$$\tilde{S}(\tilde{r}) = \frac{(x(\tilde{r}) - d)^2}{b^2} + \frac{(y(\tilde{r}))^2}{b^2} + \frac{(z(\tilde{r}) + c)^2}{a^2} - 1 = 0 \tag{5}$$

equivalent to

$$\Phi(\boldsymbol{r}) = \frac{(A_1(\boldsymbol{r}) - d)^2}{b^2} + \frac{(A_2(\boldsymbol{r}))^2}{b^2} + \frac{(A_3(\boldsymbol{r}) + c)^2}{a^2} - 1 = 0 \tag{6}$$

where

$$A_1(\boldsymbol{r}) = A_1(x, y, z) = x \cos a_1 \cos a_2 + y \sin a_1 - z \cos a_1 \sin a_2$$
$$A_2(\boldsymbol{r}) = A_2(x, y, z) = -x \sin a_1 \cos a_2 + y \cos a_1 + z \sin a_1 \sin a_2$$
$$A_3(\boldsymbol{r}) = A_3(x, y, z) = x \sin a_2 + z \cos a_2$$

Once the surface is known, the reflection point and the normal to the surface at this point can be calculate. The beam path is given by the equation for r_{beam}

$$r_{beam} = \kappa v + r_l \tag{7}$$

where r_l is the initial launching position (see Figure 4) and $\kappa \in \Re$. In particular, at the reflection point, we have

$$r_c = \kappa_c v + r_l \tag{8}$$

The substitution of (8) in (6) gives a simple equation for κ_c :

$$c_0 \kappa_c^2 + c_1 \kappa_c + c_2 = 0 \tag{9}$$

with

$$c_0 = \frac{A_1{}^2(v) + A_2{}^2(v)}{b^2} + \frac{A_3{}^2(v)}{a^2}$$

$$c_1 = 2\left(\frac{A_1(v)(A_1(r_l) - d) + A_2(v)A_2(r_l)}{b^2} + \frac{A_3(v)(A_3(r_l) + c)}{a^2} \right)$$

$$c_2 = \frac{(A_1(r_l) - d)^2 + A_2{}^2(r_l)}{b^2} + \frac{(A_3(r_l) + c)^2}{a^2} - 1$$

Equation (9) has two roots, corresponding to the two intersection points between the ellipsoid and a straight line in space representing the beam. We are only interested in one root, the one for which the beam reaches the mirror. Therefore, from Figure 7, the desired root corresponds to the bigger value of κ_c.

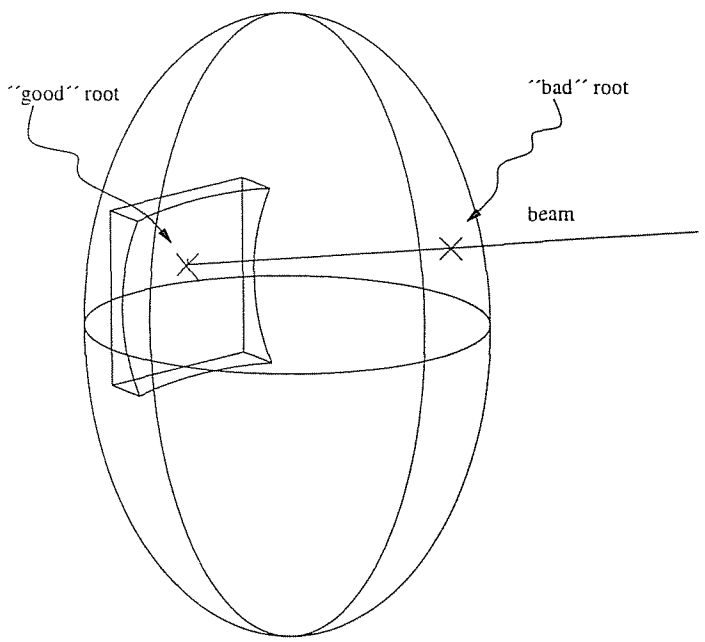

Figure 7. Roots of equation (9)

The beam hits the mirror at

$$\kappa_c = \frac{-c_1 + \sqrt{c_1^2 - 4c_0c_2}}{2c_0} \tag{10}$$

Finally, the normal vector is obtained by taking derivatives in (6)

$$\boldsymbol{N} = \frac{\nabla\Phi}{|\nabla\Phi|} = \frac{1}{|\nabla\Phi|}\left(\frac{\partial\Phi}{\partial x}, \frac{\partial\Phi}{\partial y}, \frac{\partial\Phi}{\partial z}\right)$$

$$\frac{\partial\Phi}{\partial x} = \frac{2}{b^2}[A_1(\boldsymbol{r}) - d]\cos a_1 \cos a_2 - \frac{2}{b^2}A_2(\boldsymbol{r})\sin a_1 \cos a_2 + \frac{2}{a^2}[A_3(\boldsymbol{r}) + c]\sin a_2$$

$$\frac{\partial\Phi}{\partial y} = \frac{2}{b^2}[A_1(\boldsymbol{r}) - d]\sin a_1 + \frac{2}{b^2}A_2(\boldsymbol{r})\cos a_1$$

$$\frac{\partial\Phi}{\partial z} = -\frac{2}{b^2}[A_1(\boldsymbol{r}) - d]\cos a_1 \sin a_2 + \frac{2}{b^2}A_2(\boldsymbol{r})\sin a_1 \sin a_2 + \frac{2}{a^2}[A_3(\boldsymbol{r}) + c]\cos a_2$$

Since $\boldsymbol{N}$ is the normal vector to the ellipsoid at any point $\boldsymbol{r}$,

$$\boldsymbol{w} = -\boldsymbol{N}(\boldsymbol{r}_c) \tag{11}$$

And from equation (2) we obtain the reflected beam vector $\boldsymbol{u}$ in the O-reference system.

In the limit of large a and b, the elliptic mirror becomes a plane mirror and the corresponding normal vector must be recovered. This vector has always the same components independently of the position of the reflection point. In particular, when both angles are zero, the normal vector is $\boldsymbol{w}_{pl}$ = (1,0,0) and its transformed is directly obtained from equation (3).

$$\tilde{\boldsymbol{w}}_{pl} = M\boldsymbol{w}_{pl} = (\cos a_1 \cos a_2, \sin a_1, -\cos a_1 \sin a_2)$$

The vector $\boldsymbol{u}$ is also independent of the position of the reflection point. In the limit of large a and b, the vector $\boldsymbol{w}$ given by (11) coincides with $\tilde{\boldsymbol{w}}_{pl}$.

Once $\boldsymbol{u}(a_1, a_2)$ is known the problem of finding the mirror angles for a given heating point is solved as follows. First $\boldsymbol{u}$ and $\boldsymbol{r}_c$ must be transformed to the TJ-II coordinate system. Both systems are rotated one respect to the other in the horizontal plane (xy plane) by an angle ($\pi - \varphi_{A6} = \varphi = 25.47°$). The position of the fixed point O with respect to the machine center is given by $\boldsymbol{r}_o$. The relative position of both reference systems is shown in Figure 8. The origin of the TJ-II reference system is the point $O_{TJ\text{-}II}$.

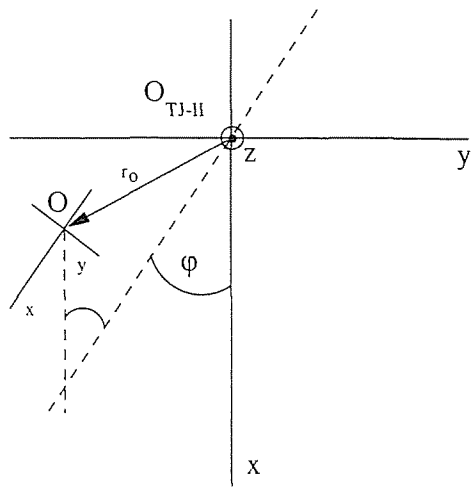

Fig.8. Coordinates transformation

Therefore the new coordinates will be given by

$$\begin{pmatrix} x_{TJ-II} \\ y_{TJ-II} \\ z_{TJ-II} \end{pmatrix} = \overbrace{\begin{pmatrix} \cos\varphi & \sin\varphi & 0 \\ -\sin\varphi & \cos\varphi & 0 \\ 0 & 0 & 1 \end{pmatrix}}^{R} \begin{pmatrix} x \\ y \\ z \end{pmatrix} + \boldsymbol{r_o} \quad ; \quad \boldsymbol{r_o} = \begin{pmatrix} 1140{,}2\ \text{mm} \\ -631{,}7\ \text{mm} \\ 613{,}9\ \text{mm} \end{pmatrix}$$

and $\boldsymbol{u}_{TJ-II} = R\boldsymbol{u}$. If we want the reflected beam to go through an arbitrary point $\boldsymbol{r_a}$ somewhere in the plasma, the direction of the beam will be given by (see Figure 9)

$$\hat{\boldsymbol{u}} = \frac{\boldsymbol{r_a} - \boldsymbol{r}_{c,TJ-II}}{\left|\boldsymbol{r_a} - \boldsymbol{r}_{c,TJ-II}\right|} \tag{12}$$

where $\boldsymbol{r}_{c,TJ-II} = R\boldsymbol{r}_c + \boldsymbol{r}_o$

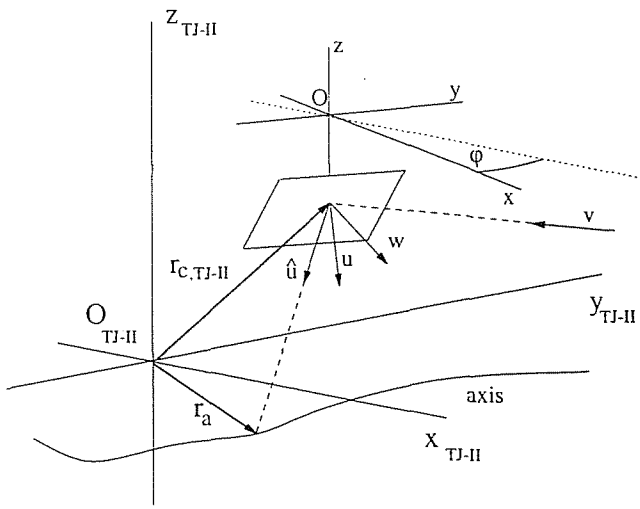

Figure 9.Calculation of the positioning angles in the TJ-II reference system. In this particular case, r_a is located on the magnetic axis

The desired angles will be the solution of

$$\hat{u} \cdot u_{TJ-II} = 1 \tag{13}$$

This equation is solved defining a functional F and finding the angles a_1 and a_2 that minimizes F, these angles will be the solution of (13).

$$F(u_{TJ-II}(a_1, a_2), \hat{u}(a_1, a_2)) \equiv u_{TJ-II} \cdot \hat{u} - 1 \tag{14}$$

The movement of the mirror, and hence the direction of the reflected beam is limited physically by the vacuum vessel. Anyway, due to the fact that the plasma has a strong helical structure, big angles in the toroidal direction could send the reflected beam to the vessel walls without contact the plasma. Moreover, the strong magnetic field dependence on the machine toroidal and poloidal angles provides a wide range of attainable values for the parallel index of refraction $N_{||} = (c/w|\mathbf{B}|)\mathbf{k}.\mathbf{B}$

4.Heating on-axis

Depending on the values of the angles, the system is capable of localized on-axis power deposition at different toroidal positions, each one with different fraction of trapped particles. In particular, for r_a located along the magnetic axis (see Figure 9), the results obtained are shown in Figures 10a and 10b. The computation of the normalized magnetic flux used in the calculation of the magnetic axis position has been performed by fitting the magnetic flux surfaces with a neural network [5]. The values of the angles a_1 and a_2, measured in degrees, for which the beam hits the magnetic axis are represented as a function of $N_{||}$ in Figure 10a and as a function of the machine toroidal angle in Figure 10b for a given magnetic configuration. As noted before the values of $N_{||}$ cover a wide range, from $N_{||} = -0.8$ to $N_{||} = 0.8$. A detailed study of the heating flexibility together with ECCD simulations in TJ-II can be found in ref [4].

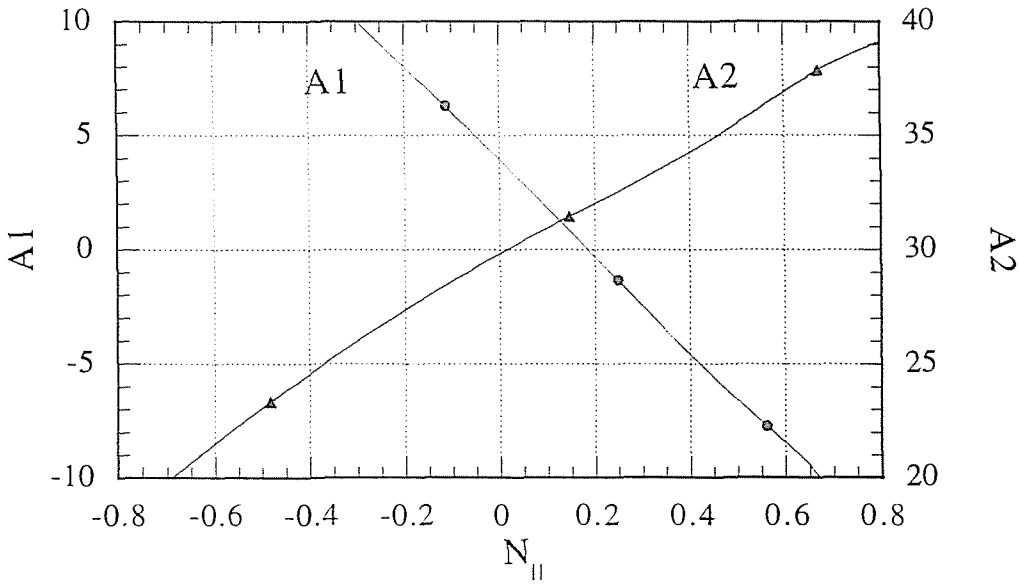

Figure 10a. Angles a_1 and a_2 vs $N_{||}$

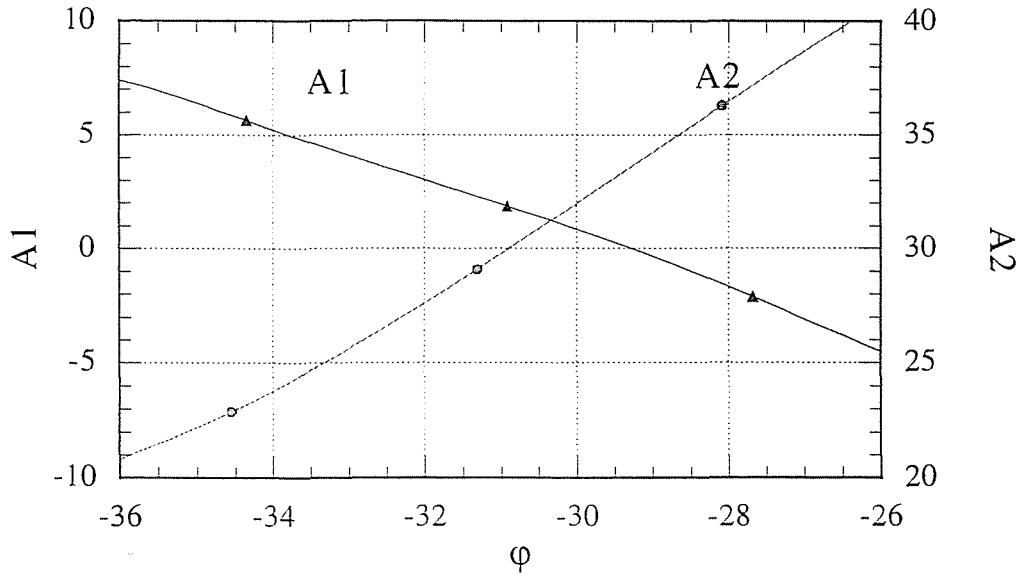

Figure 10b. Angles a_1 and a_2 vs TJ-II toroidal angle. The origin is taken at $\varphi = 90°$ (see Figure 1)

5.Mirror calibration

5.1 Experimental set-up

The mirror was calibrated in laboratory with a special stand on an optical bench. The whole body of the mirror window flange (with the mirror installed in it) was used as reference for the alignment of a laser beam. Once aligned the beam was directed towards the mirror center to find the drives zero position (where $a_1 = a_2 = 0°$). A screen with a hole in it, allowing the laser beam to go through, was placed in front of the mirror to receive the reflected beam for different mirror positions. Moreover, a vertical reference metallic plate was placed on the stand behind the mirror to measure the poloidal angles by mechanical means using a protractor. The whole set-up is shown in Figure 11.

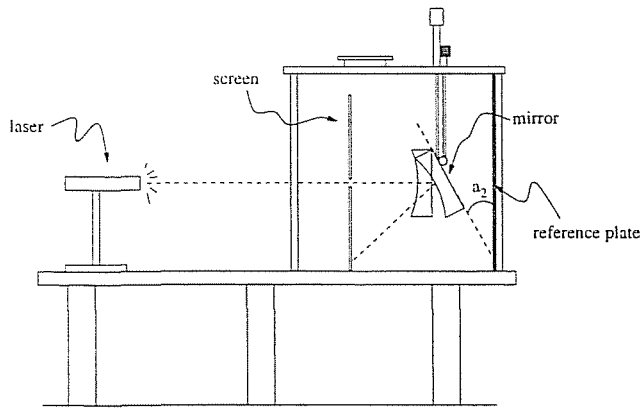

Figure 11. Experimental set-up

5.2 Measurements

As explained in Section 2, the mirror is handled by two drives, a rotary drive for a_1 and a linear drive for a_2. First, the toroidal range was measured, keeping $a_2 = 0°$. In this case

the spatial position of the center of the mirror surface is practically constant for small values of a_1. The lack of precision in the position of the reflected spot in the screen, due to the roughness of the mirror surface, hinders the measurements and makes very difficult the error estimation. For that reason, the dependence on a_1 of the position of the center of the mirror is not considered and no error calculation could be done. Only an average reliable error is considered. The angle a_1 is obtained directly from the distance measured on the screen. A range wider than necessary was measured and the results are shown on Table 1.

As we know from Section 3, the distance from the screen to the mirror, along the laser beam path, is clearly dependent on the value of a_2, then the displacement distance of the spot measured in the screen is not directly related with the angle. This, an also the fact that the mirror is elliptical, has to be taken into account by using the results of Section 3 when reconstructing the angle a_2 from the screen measurements. Nevertheless, the precision problem mentioned above becomes critical in the relevant operation range, going approximately from a_2 =20° to a_2 =35°, and the optical measurements can not be done with the described experimental set-up so poloidal angles are measured directly by mechanical means. The poloidal measurements precision is higher than the precision obtained for the toroidal angles since the mechanical measurements were easier to perform (unfortunately, the toroidal angles could only be measured using the laser beam). The measurements are shown on the table and in figs.12a and 12b. The design requirements, strongly affected by the lack of space inside the machine, produce a weak non-linear dependence of the angles on the values displayed in the drives and an asymmetry between negative and positive values of a_1.

Toroidal angles			Poloidal angles	
divisions Δ=±.5 div	a_1(deg) Δ=±0,6°	a_1(deg) Δ=±0,6°	divisions Δ=±.5 div	a_2(deg) Δ=±0,2°
2	-0,6	1,6	14	22,0
3	-1,8	2,8	15	23,5
4	-3,3	3,9	16	25,0
5	-4,7	5,1	17	26,5
6	-6,0	6,4	18	27,7
7	-7,3	7,9	19	29,5
8	-7,9	8,8	20	31,0
9	-8,7	9,9	21	32,1
10	-10,1	10,8	22	33,5
11	-11,3	11,9	23	34,9
12	-12,5	12,8	24	36,2
13	-13,3	13,9	25	37,3
14	-13,9	14,9	26	38,4
15	-14,9	15,7	27	39,6
16	-15,7	16,7	28	40,5
17	-16,3	17,6	29	41,7
18	-17,1	18,5	30	42,8
19	-17,8	19,0	31	43,7
20	-18,8	19,6	--	--
21	-19,6	20,8	--	--
22	-19,9	21,0	--	--
23	-20,3	21,3	--	--

Table1. Measured toroidal and poloidal angles

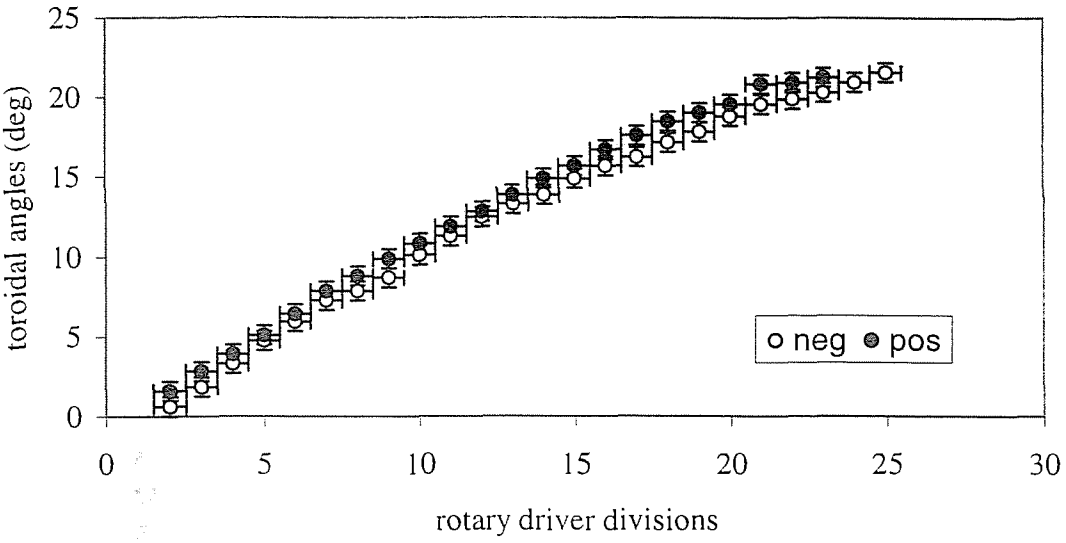

Figure 12a. Measured toroidal angles

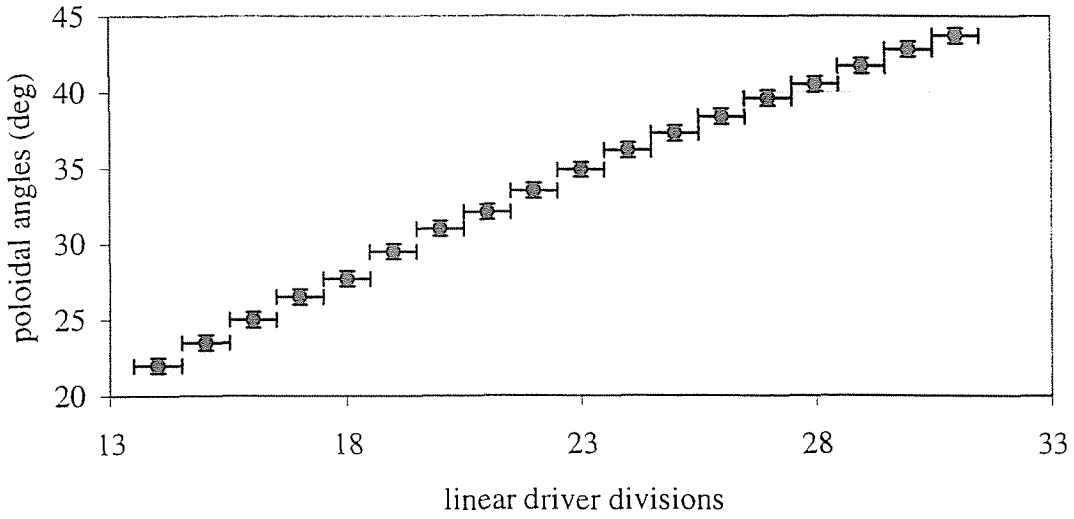

Figure 12b. Measured poloidal angles

Conclusions

The internal mirror located at the end of each transmission line allows us to modify the position of the heating point. The calculation of the mirror positioning angles for which the microwave beam goes through this point has been presented and the particular case of on-axis power deposition has been considered. The precision of the measurements done in laboratory is good enough to ensures the use of this mirror as an appropriate tool for ECRH and ECCD experiments. The lack of space inside the vessel is the main responsible for the complication in the mirror movement design and hence in the calculations. A future design should consider a rotation around the central point of the mirror surface so the direction of the reflected beam will be obtained straightforward.

Appendix 1

As explained in Section 3 the mirror moves around two axis, the $\tilde{z}$ axis, belonging to the mirror itself, and the y axis which is a fixed axis belonging to the $\{O, x, y, z\}$ reference system. The matrix M was calculated supposing that the rotation R_1 of the arbitrary vector $\boldsymbol{r}$, represented by M_1, around the mirror axis, was applied first, so the axis $\tilde{z}$ and z were still the same. Thus, the second rotation R_2 applied on $\boldsymbol{r}'$, was around the y axis. The result was that both rotations were around fixed reference axis and the two matrices representing these rotations could be obtained straightforward.
If the order is inverted and R_2 is applied first, the second rotation R_1 is around $\tilde{z}$, which now differs from the fixed reference axis z, and the matrix representing this last rotation is more complicated than was M_2 in the previous case. To calculate the expression of the new matrix M_n in the $\{O, x, y, z\}$ system we define an intermediate coordinate system $\{O, x_{int}, y_{int}, z_{int}\}$ which is the transformed by R_2 of the system $\{O, x, y, z\}$ (see Figure 13). The advantage is that the rotation M_n, referred to this system, takes a well-known matrix expression, that is M_1

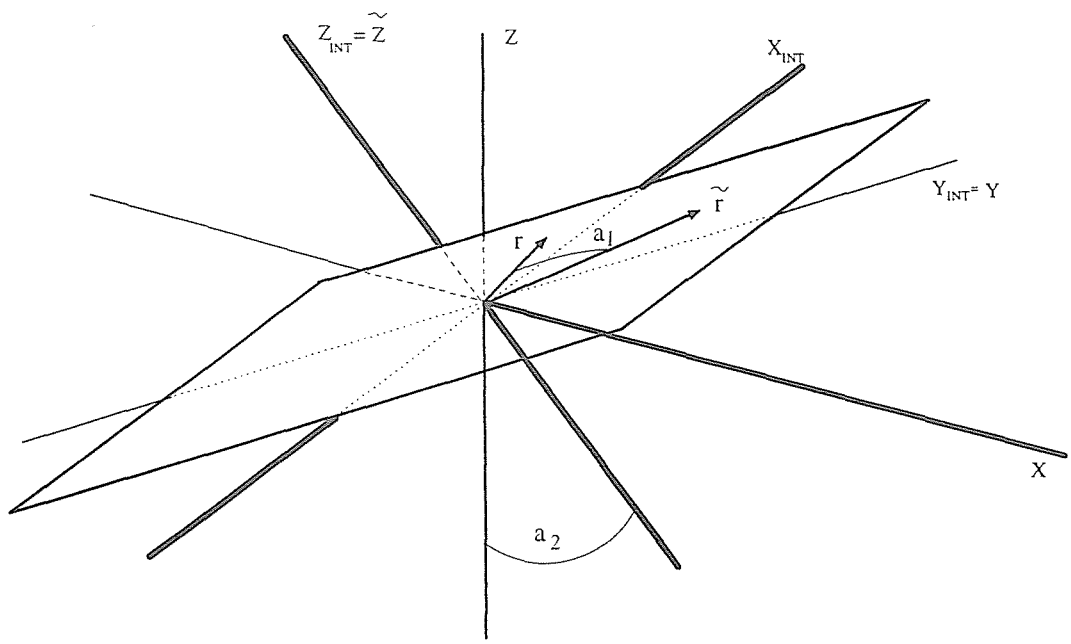

Fig 13.The intermediate coordinates system

$$\begin{pmatrix} \tilde{x}_{\text{int}} \\ \tilde{y}_{\text{int}} \\ \tilde{z}_{\text{int}} \end{pmatrix} = \overbrace{\begin{pmatrix} \cos a_1 & -\sin a_1 & 0 \\ \sin a_1 & \cos a_1 & 0 \\ 0 & 0 & 1 \end{pmatrix}}^{M_n^{\text{int}} = M_1} \begin{pmatrix} x'_{\text{int}} \\ y'_{\text{int}} \\ z'_{\text{int}} \end{pmatrix} \tag{1}$$

Since R_2 is a rotation around the y axis the coordinates transformation will be given by

$$\begin{pmatrix} x_{\text{int}} \\ y_{\text{int}} \\ z_{\text{int}} \end{pmatrix} = \begin{pmatrix} \cos a_2 & 0 & -\sin a_2 \\ 0 & 1 & 0 \\ \sin a_2 & 0 & \cos a_2 \end{pmatrix} \begin{pmatrix} x \\ y \\ z \end{pmatrix} = M_2^{-1} \boldsymbol{r} \tag{2}$$

and combining (1) with (2) we obtain

$$\begin{pmatrix} \cos a_2 & 0 & -\sin a_2 \\ 0 & 1 & 0 \\ \sin a_2 & 0 & \cos a_2 \end{pmatrix} \begin{pmatrix} \tilde{x} \\ \tilde{y} \\ \tilde{z} \end{pmatrix} = \begin{pmatrix} \cos a_1 & -\sin a_1 & 0 \\ \sin a_1 & \cos a_1 & 0 \\ 0 & 0 & 1 \end{pmatrix} \begin{pmatrix} \cos a_2 & 0 & -\sin a_2 \\ 0 & 1 & 0 \\ \sin a_2 & 0 & \cos a_2 \end{pmatrix} \begin{pmatrix} x' \\ y' \\ z' \end{pmatrix}$$

or

$$\begin{pmatrix} \tilde{x} \\ \tilde{y} \\ \tilde{z} \end{pmatrix} = \underbrace{\begin{pmatrix} \cos a_2 & 0 & -\sin a_2 \\ 0 & 1 & 0 \\ \sin a_2 & 0 & \cos a_2 \end{pmatrix}^{-1} \begin{pmatrix} \cos a_1 & -\sin a_1 & 0 \\ \sin a_1 & \cos a_1 & 0 \\ 0 & 0 & 1 \end{pmatrix} \begin{pmatrix} \cos a_2 & 0 & -\sin a_2 \\ 0 & 1 & 0 \\ \sin a_2 & 0 & \cos a_2 \end{pmatrix}}_{M_n} \begin{pmatrix} x' \\ y' \\ z' \end{pmatrix}$$

This is the usual expression for the coordinates transformation of any mathematical operator. Since $\boldsymbol{r}' = M_2 \boldsymbol{r}$, then

$$\tilde{\boldsymbol{r}} = M_n \boldsymbol{r}' = M_n M_2 \boldsymbol{r} = N\boldsymbol{r}$$

$$M_n = \left(M_2^{-1}\right)^{-1} M_1 M_2^{-1}$$

and

$$N = M_n M_2 = \left(M_2^{-1}\right)^{-1} M_1 \overbrace{M_2^{-1} M_2}^{\mathbf{I}} = M_2 M_1 = M$$

As expected, both matrices M and N are the same and the calculation done in Section 3 is the shortest and the simplest one.

References

[1] **R. Martín et al**. 'Complex for ECRH and ECCD experiments on TJ-II'. Proceedings of the 20th SOFT, September 1998, Marseille. P 403.
[2] **A. Fernández, K. Likin, R. Martín.**, and **A. Cappa**. 'Quasi-optical Transmission Lines for ECRH on TJ-II Stellarator'. Informes Técnicos Ciemat (to be published).
[3] **A. Fernández, K. Likin, R. Martín**. 'Advanced Design of the first Quasi-optical Transmission Line for ECRH at TJ-II'. Informes Técnicos Ciemat **889**
[4] **V. Tribaldos, J.A. Jimenez, J. Guasp and B. Ph. van Milligen**. 'Electron cyclotron heating and current drive in the TJ-II stellarator'. Plasma Phys. Control. Fusion **40** (1998) P 2113-2130
[5] **V. Tribaldos and B. Ph. van Milligen.** 'Neural network for rapid recovery of plasma topology'. Review of Scientific Instruments **68** (1997) P 931.

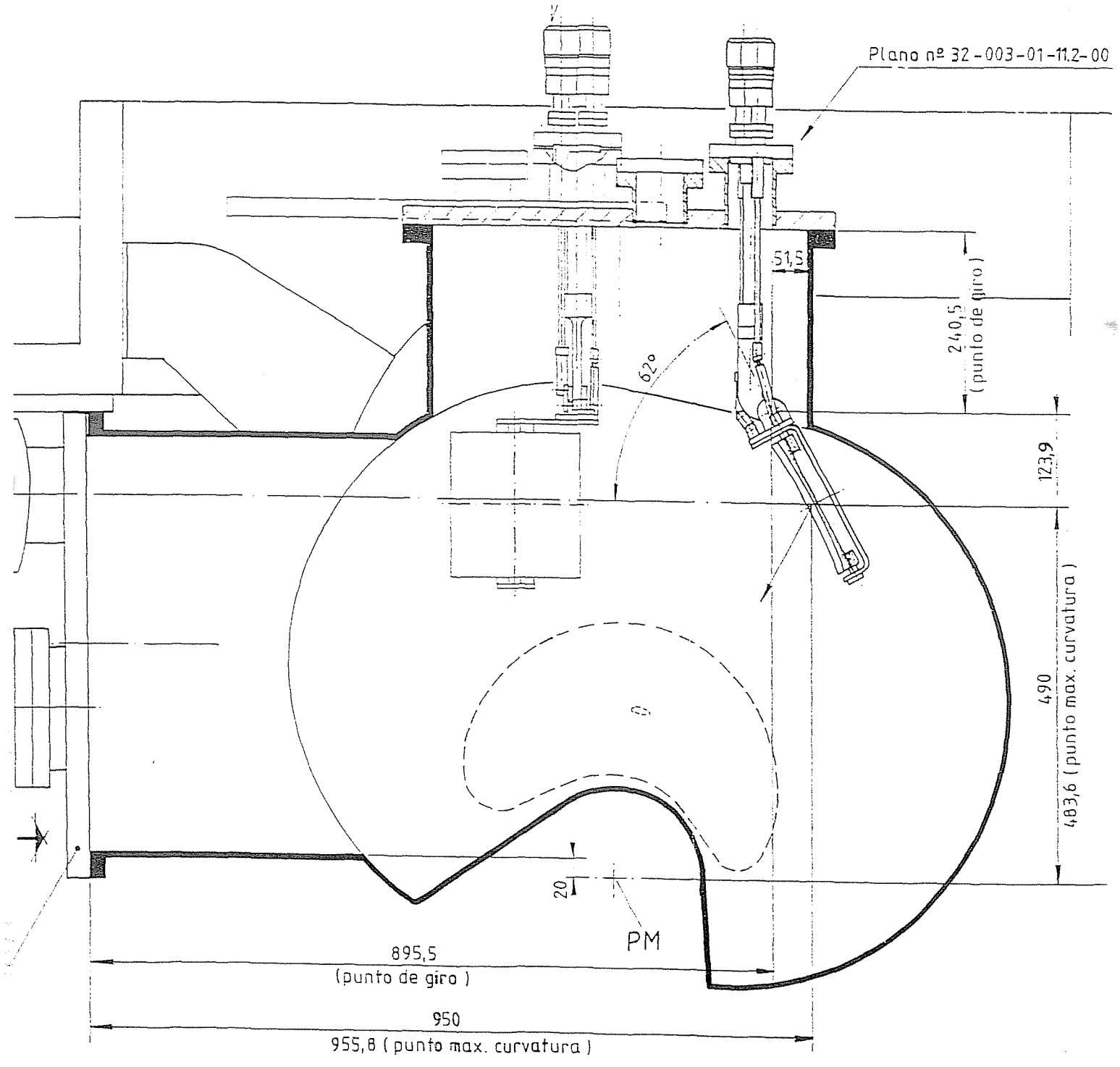
Plano nº 32-003-01-11.2-00
51,5
240,5
(punto de giro)
62°
123,9
490
483,6 (punto max. curvatura)
20
PM
895,5
(punto de giro)
950
955,8 (punto max. curvatura)